Multiscale Modeling of Rising Packed Bubbles

Kazuyasu, SUGIYAMA*, Shu TAKAGI** and Yoichiro MATSUMOTO**

**Intelligent Modeling Laboratory, The University of Tokyo*

1-1-1Yayoi, Bunkyo-ku, Tokyo, 113-8656, JAPAN

***Department of Mechanical Engineering, The University of Tokyo*

7-3-1 Hongo, Bunkyo-ku, Tokyo, 113-8656, JAPAN

Bubbly flow has multiple structures in time and spatial scales. The macro-scale flow structure in multi-phase flow is affected by the micro-scale phenomena and also mezzo-scale ones. The two-fluid model based on the volume average of the governing equations for two-phases is often used for the industrial applications. However, the Sub-Grid Scale (SGS) phenomena related to the mezzo-scale phenomena have been neglected in the conventional studies by the two-fluid model. In the present study, the multiscale modeling of the rising packed bubbles is conducted. The Direct Numerical Simulation (DNS) are carried out and some averaged quantities are extracted from the result. The bubbles are spherical ones with no-slip boundary condition, which correspond to the sub-mm scale diameter bubbles in the contaminated water. A periodic box is used for the simulation to extract the turbulence in the bubbly flow. The two-fluid simulation is also carried out at the same condition as the present DNS. Constitutive equations, where not only SGS stresses but also boundary conditions of the pressure and the vorticity on the interface are taken into account, are derived for the averaged equations. The turbulent energy spectrum obtained by the present two-fluid model reproduces the DNS result well, while the result by the conventional two-fluid model, where the SGS stress and the boundary conditions on the interface are neglected, show considerable difference with the DNS one.

1. Introduction

The bubbly flow is often observed in many industrial fields, such as chemical plants, bio-reactors, and nuclear power plants. The bubbly flow contains the several characteristic length scales, from a bubble diameter (micro-scale) to the large flow structure (macro-scale). As many researchers reported, the flow structure is altered by the injection of air bubbles, and the multi-scale structure of the bubbly flow plays important role on the flow modulation. The mezzo-scale phenomena in a bubbly flow, which are related to the bubble-bubble interaction, play an important role on the turbulence induced by the bubble motion.

By using the DNS, where the multi-scale phenomena of the bubbly flow are considered, we can predict the detailed flow structure. However, a lot of numerical resources are consumed in the DNS and most of the engineering simulations are unrealistic. Considering the industrial applications, the two-fluid model based on the volume-averaged equations (Ishii, 1975; Drew, 1983; etc.) is useful and many researchers have carried out the bubbly flow simulations by the two-fluid approach (Matsumoto *et al*., 1988; Murai & Matsumoto, 1996; etc.). In such the method, the conservation equations are directly derived from the Navier-Stokes equation so that the two-phase interaction due to the inertia difference may be adequately solved. The two-fluid model is derived by the filter operation in the same manner as the Large Eddy Simulation (LES), thus some SGS closure problems are appeared. However, the SGS phenomena related to the mezzo-scale phenomena have been neglected in the conventional studies by the two-fluid model due to the lack of knowledge about them. Therefore, the system of the conventional two-fluid approach is not adequate to analyze the bubble-bubble or bubble-liquid interaction and it is not appropriate for the analysis of the mezzo-scale phenomena of the bubbly flow.

In the present study, the mezzo-scale phenomena of the bubbly flow are numerically studied and some constitutive equations for the multiscale modeling are derived. The DNS of the rising packed bubbles is carried out and some averaged quantities are extracted from the result. The two-fluid simulation is also carried out in the same condition as the present DNS and the ability of constitutive equations for the SGS modeling is discussed.

2. Assumptions

In the present study, the following assumptions are employed to formulate the governing equations: (1) Bubble maintains a spherical shape. (2) Change of bubble volume is not considered. (3) The water is contaminated. Hence, a no-slip boundary condition is imposed on a bubble surface. (4) Coalescence of bubbles is not considered. (5) Bubble-bubble collision is elastic.

3. Direct Numerical Simulation (DNS)

In order to obtain the detained information of the turbulent structure in the bubbly flow, the DNS of the packed bubbles in the periodic box is carried out.

3.1 Governing equations

Mass conservation equation:

$$\frac{\partial u_{fi}}{\partial x_i} = 0. \tag{1}$$

Momentum conservation equation:

$$\frac{\partial \rho_k u_{ki}}{\partial t} + \frac{\partial \rho_k u_{ki} u_{kj}}{\partial x_j} = \frac{\partial}{\partial x_j}\left\{-\delta_{ij}p + \mu_k\left(\frac{\partial u_{ki}}{\partial x_j} + \frac{\partial u_{kj}}{\partial x_i}\right)\right\} + (\rho_k - \rho_f)g_i. \tag{2}$$

Equation of translational motion of a bubble:

$$\frac{4\pi r_p^3 \rho_p}{3}\frac{du_{pi}}{dt} = \int_{r=a} dS\left\{-\delta_{ij}p + \mu\left(\frac{\partial u_{fi}}{\partial x_j} + \frac{\partial u_{fj}}{\partial x_i}\right)\right\} n_j + \frac{4\pi r_p^3}{3}(\rho_p - \rho_f)g_i \tag{3}$$

Equation of angular momentum of a bubble:

$$\frac{8\pi r_p^5 \rho_p}{15}\frac{d\omega_{pi}}{dt} = \int_{r=a} dS\epsilon_{ijk}r_j\left\{\mu\left(\frac{\partial u_{fk}}{\partial x_l} + \frac{\partial u_{fl}}{\partial x_k}\right)\right\} n_l. \tag{4}$$

3.2 Simulation method

The algorithm to solve governing equations is same as our previous study (Sugiyama *et al*., 2000). The finite difference method (FDM) is employed to solve the partial differential equations. The grid size is smaller than the bubble diameter. Using the regular rectangular grid system, the no-slip boundary condition on a bubble surface is approximated. The spatial derivative terms are approximated by the fourth-order central scheme. The time integral of the flow velocity is conducted in the fourth-order Runge-Kutta method. In terms of the time integral procedures of the translational bubble motion, the second-order Crank-Nicholson method and Adams-Bashforth method are employed for the bubble position and the bubble velocity, respectively.

3.3 Simulation conditions

The simulation parameters are the void fraction (f_G). The bubble radius (a), the kinematic viscosity (ν) and the gravity (g) are 0.25(mm), 1.0×10^{-6}(m^2/s) and -10(m/s^2), respectively. The simulation conditions are shown in Table 1.

Table 1 Simulation conditions of multi-bubble motion

	Domain size	Number of grid
Case1	$4.0^3(\mathrm{mm}^3)$	64^3
Case2	$8.0^3(\mathrm{mm}^3)$	128^3

3.4 Instantaneous flow structure

Figure 1 shows that the instantaneous flow structure of the bubble position and the pressure distribution with the variety of the void fraction of 0.833, 3.33 and 10.0(%). As shown in Fig. 1, in the higher void fraction, the pressure contour distorts more strongly in the horizontal direction. Such a distorted pressure contour indicates that the strong bubble-bubble interaction is occurred.

In order to estimate the turbulent structure of the bubbly flow, Fig. 2 shows the one-dimensional vertical energy spectrum at the void fraction (f_G) of 0.833(%). $E_{11}(k_1)$ and $E_{22}(k_2)$ indicate vertical and horizontal components, respectively. Symbols and lines in Fig. 2 correspond to the results of case1 and case2, respectively. As shown in Fig. 2, the both results of case1 and case2 agree well each other, thus domain size of case1 is considered to be large enough to obtain the turbulent structure induced by the motion of bubbles. It is seen from Fig. 2 that the vertical energy spectrum ($E_{11}(k_1)$) is much larger than the horizontal one ($E_{22}(k_2)$) for all conditions since the turbulent structure of the bubbly flow is inhomogeneous.

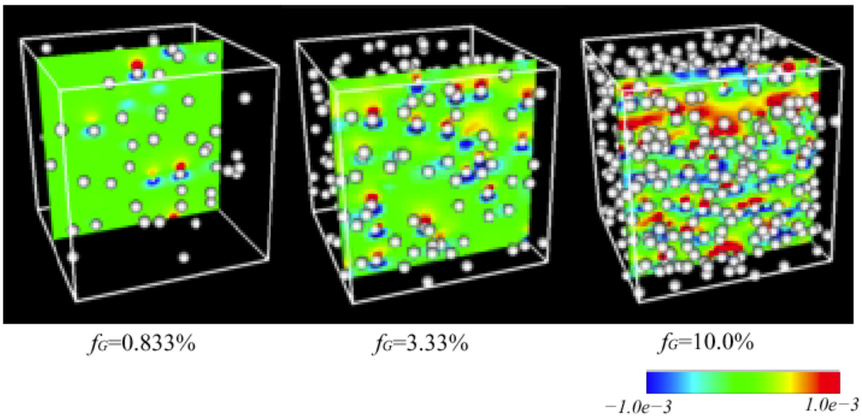

Fig. 1 Instantaneous bubbles and pressure distributions (case2)

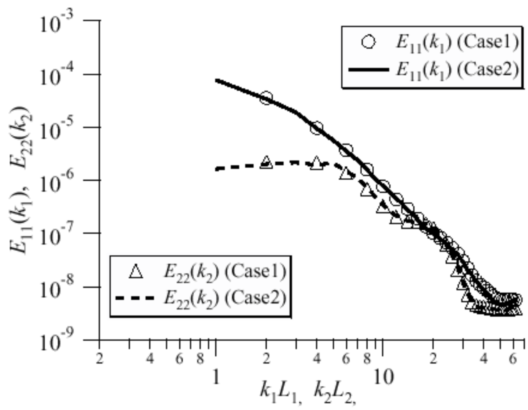

Fig. 2 One-dimensional vertical energy spectrum distribution versus wave number.(f_G=0.833 (%), case1 and case2)

3.5 Local SGS stresses induced by bubble motion

The most of numerical studies of the bubbly flow have been based on the two-fluid approach using the volume averaged equations. It is wellknown that the SGS stress (or the Reynolds stress) terms are appeared by averaging the non-linear terms. However, these terms has been often neglected in the two-fluid simulation. We previously conducted so-called '*a priori* study' of the closure problem for the SGS stress of the bubbly flow. We investigated the correlation between some model SGS stresses used in the LES of the single phase flow and the actual SGS stress obtained by the result of the DNS (Sugiyama *et al.*, 2000). The results showed that the model stress based on the non-linear model ($\tau_{ij}^{(\mathrm{Model})*}$, Liu *et al.*, 1994) had higher correlation (more than 0.9 at the void fraction of 0.833(%)) with the actual SGS stress (τ_{ij}^{*}) than the model stresses based on the Smagorinsky (1963) model and the scale similarity model (Bardina *et al.*, 1983). The actual SGS stress and the present model stress are expressed as

$$\begin{aligned}\tau_{ij}^{*} &= -\left(\frac{\langle X_L u_i u_j\rangle}{\langle X_L\rangle} - \frac{\langle X_L u_i\rangle\langle X_L u_j\rangle}{\langle X_L\rangle^2}\right)^{*}, \\ &= -(\overline{u_{Li}u_{Lj}} - \bar{u}_{Li}\bar{u}_{Lj})^{*},\end{aligned} \tag{5}$$

$$\tau_{ij}^{(\mathrm{Model})*} = -\left(\frac{\overline{\Delta}^2}{12}\left(\sum_{\text{All Bub.}}\frac{\partial u_i^{(PI)}}{\partial x_k}\right)\left(\sum_{\text{All Bub.}}\frac{\partial u_j^{(PI)}}{\partial x_k}\right)\right)^{*}, \tag{6}$$

where <> is the grid filter operation with the grid size Δ, X_L is the indicator function of 1 at liquid and 0 at gas, the superscript * indicates the anisotropic tensor and $\bar{\ }$ is the phase volume averaging. In Eq. (6), the velocity gradient is analytically calculated by using the database of the mean velocity field around bubbles $u_i^{(PI)}$. The velocity field induced by the bubble motion is written by the poloidal vector field (Chandrasekhar, 1961) under the assumption that the mean velocity field is axisymmetric. The velocity field around bubbles is expanded by the spherical harmonics and the polynomials. The radial and tangential components of the velocity are expressed as

$$u_r^{(PI)}(r,\theta,Re) = \sqrt{\frac{4\pi}{3}}|u_G - u_L^{\infty}|\sum_{n=1}^{N}\sum_{m=1}^{M}\tilde{u}_{nm}^{(r)}(Re)a^m r^{-m}Y_n(\theta), \tag{7}$$

$$u_\theta^{(PI)}(r,\theta) = \sqrt{\frac{4\pi}{3}}|u_G - u_L^{\infty}|\sum_{n=1}^{N}\sum_{m=1}^{M}\frac{m-2}{\sqrt{2n(n+1)}}\tilde{u}_{nm}^{(r)}a^m r^{-m}Y_{n1}(\theta). \tag{8}$$

where $|u_G-u_L^{\infty}|$ is the relative velocity of the bubble to the liquid and $u_{nm}(r)$ is the coefficient of the spherical harmonics/polynomials expansion. By using the orthogonal relation of the spherical harmonics, the expansion for the θ-direction is carried out. For the r-direction, the polynomials expansion is carried out by the least squire method for a finite domain ($a<r< 6a$).

4. Two-Fluid Simulation (Effect of SGS Stress)

In the present section, we discuss the effect of the SGS stress, which has been neglected in the conventional two-fluid simulation. The two-fluid simulation with the SGS model given by Eq. (6) is carried out at the same conditions as the DNS and so-called '*a posteriori* study' is conducted. The governing equations and the simulation procedures are almost based on the Euler-Lagrange model developed by Murai and Matsumoto (1996).

4.1 Governing equations

Conservation equation of gas volume fraction:

$$\frac{\partial f_G}{\partial t} + \frac{\partial f_G\overline{u_{Gi}}}{\partial x_i} = 0, \tag{9}$$

Conservation equation of liquid volume fraction:

$$\frac{\partial f_L}{\partial t} + \frac{\partial f_L \overline{u_{Li}}}{\partial x_i} = 0. \tag{10}$$

Restriction condition of volume fraction:

$$f_G + f_L = 1. \tag{11}$$

Momentum conservation equation of mixture fluid:

$$\frac{\partial f_L \overline{u_{Li}}}{\partial t} + \frac{\partial f_L \overline{u}_{Li} \overline{u}_{Lj}}{\partial x_j} = -\frac{1}{\rho_L}\frac{\partial p}{\partial x_i} + \frac{\partial}{\partial x_j}\frac{\mu}{\rho_L}\frac{\partial \overline{u_{Li}}}{\partial x_j} + \frac{1}{3}\frac{\partial}{\partial x_i}\frac{\mu}{\rho_L}\frac{\partial \overline{u_{Lj}}}{\partial x_j} - f_G g_1 + \frac{\partial}{\partial x_j}(f_L \tau_{ij}), \tag{12}$$

where the inertia effect of the gas phase is neglected using the relation of ρ_G/ρ_L<<1 and τ_{ij} is the SGS stress of the bubbly flow given by Eq. (5). The formula of the effective viscosity for the dilute suspension containing rigid spherical particles (Batchelor, 1967) is used for the viscosity of the bubbly flow.

$$\mu = (1 + 2.5 f_G)\mu_L. \tag{13}$$

Equation of a bubble translational motion:

$$\frac{1}{2}\left(\frac{d\rho_L V_G^{(l)} u_{Gi}^{(l)}}{dt} - \frac{D_L \rho_L V_G^{(l)} \overline{u_{Li}}}{Dt}\right) = V_G^{(l)}\left\{-\frac{\partial p}{\partial x_i} + \mu_L\left(\frac{\partial^2}{\partial x_j \partial x_j}\overline{u_{Li}} + \frac{1}{3}\frac{\partial^2}{\partial x_i \partial x_j}\overline{u_{Lj}}\right)\right\} - \frac{1}{2}\pi a^{(l)2}\rho_L C_D \left|u_G^{(l)} - \overline{u_L}\right| (u_{Gi}^{(l)} - \overline{u_{Li}}) - V_G^{(l)} g_1 \rho_L, \tag{14}$$

where the added inertia, pressure, drag and gravitational forces are considered, V_G is the bubble volume and C_D is the drag coefficient on the bubble. The empirical formula is adopted for C_D derived by the Schiller and Naumann (1933) and C_D is expressed as

$$C_D = \frac{24}{Re_b^{(l)}}\left(1 + 0.15 Re_b^{(l)0.687}\right), \tag{15}$$

where Re_b is the bubble Reynolds number and is expressed as

$$Re_b^{(l)} = \frac{2\rho_L a \left|u_G^{(l)} - \overline{u_L}\right|}{\mu_L}. \tag{16}$$

4.2 Simulation method

The FDM is employed to solve the partial differential equations. The spatial derivative terms are approximated by the fourth-order central scheme. The time integral of the flow velocity is conducted in the second-order Adams-Bashforth method. In terms of the time integral procedures of the translational bubble motion, the second-order Crank-Nicholson method and Adams-Bashforth method are employed for the bubble position and the bubble velocity, respectively. The interpolation from the liquid phase to the gas one is approximated by the fifth order spline method.

4.3 Simulation conditions

The box size of the simulation domain is 16**x**16**x**16 (mm^3) divided by 16**x**16**x**16 grids. We carry out two simulations: one is the conventional simulation, where the SGS stress (τ_{ij}) is 0, and the other is based on the non-linear model, where the SGS stress is given by Eq. (6).

4.4 Simulation results

Figure 3 shows the vertical component of the one-dimensional vertical energy spectra at the void fraction of 0.833%. Solid and dotted lines correspond to the DNS data without and with the grid filter operation, respectively. Symbols '△' and '○' correspond to the result of the conventional model (τ_{ij}=0) and that of the present non-linear model given by Eq. (6). It is seen from Fig. 3 that the energy spectra of the DNS with the grid filter operation is smaller than that without the grid filter operation. It is because that the turbulent structure induced by the motion of the bubbles is locally distributed near the bubbles and such the turbulence is smoothed by the grid filter operation. The averaged equations are obtained by the grid filter operation of the NS equation, thus it is desirable that the result of the two-fluid simulation agrees with that of the DNS with the grid filter operation. The both results obtained by the two-fluid model are quite underestimated compared with the DNS results. It is also seen from Fig. 3 that no significant difference between the conventional and the present non-linear models is recognized. According to the '*a priori* study' (Sugiyama *et al*., 2000), the present model stress has high correlation with the actual SGS stress and is considered to be good SGS stress model. However, the present non-linear model does not improve the difference between the conventional two-fluid model and the DNS. Therefore, for the SGS modeling of the bubbly flow, we must consider not only the SGS stress (the Reynolds stress) but also another effect. In the next section, we discuss the problem of the previous simulation method based on the two-fluid model.

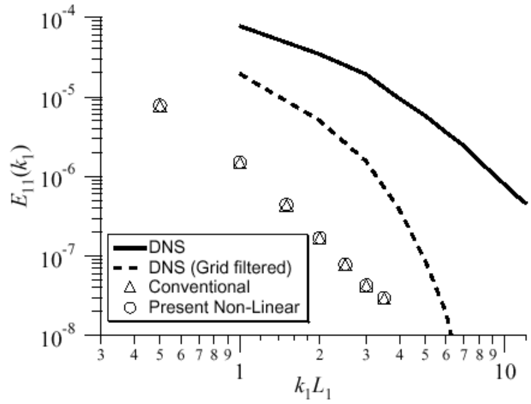

Fig. 3 One-dimensional vertical energy spectrum distribution versus wave number.(Vertical component, f_G=0.833%)

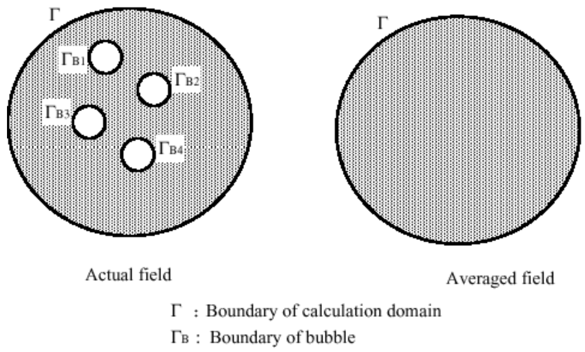

Fig. 4 Schematic of boundaries in actual and two-phase averaged fields

5. On Effects of Boundary Condition in Two-Fluid Simulation

Figure 4 shows the boundaries of the bubbly flow. The left figure shows the boundaries of the actual bubbly flow and the right one shows those considered in the averaged equations. Γ shown in Fig. 4 is the boundary of the simulation domain and Γ_{Bl} is the interface on the bubble l. In the case of the DNS, the governing equations are solved under the proper boundary conditions on the boundary of the simulation domain Γ and the bubble interface Γ_{Bl}. However, in the case of the conventional two-fluid simulation, the boundary condition on the bubble interface Γ_{Bl} was not explicitly solved. Therefore, we must consider not only the SGS stress (the Reynolds stress) but also the boundary conditions on the bubble interface for the SGS modeling. Considering the SGS stress modeling, we can find the SGS stress term in the momentum equation. On the contrary, we cannot find any boundary condition effect in the governing equations, thus we cannot conduct '*a priori* study' for the modeling of the boundary condition effect using DNS results.

In the present section, the problem what variables should be taken into account to model the boundary condition effect is made clear and the new simulation method for the incompressible bubbly flow is proposed.

5.1 Problem on pressure

The following relation is derived by Eq. (11).

$$\frac{\partial (f_G + f_L)}{\partial t} = 0. \tag{17}$$

From Eqs. (9)(10)(17), the solenoidal condition for the bubbly flow is obtained.

$$\frac{\partial (f_G \bar{u}_{Gi} + f_L \bar{u}_{Li})}{\partial x_i} = 0. \tag{18}$$

In the case of f_G =0, Eq. (18) corresponds to the solenoidal condition of the single phase flow. Using the Helmholtz decomposition, the total volume flux is expressed as

$$f_G \bar{\mathbf{u}}_{Gi} + f_L \bar{\mathbf{u}}_{Li} = \nabla \phi + \nabla \times \Psi. \tag{19}$$

where ϕ is the harmonic function ($\nabla^2\phi$=0) and $\mathbf{\Phi}$ is the vector function. In the incompressible bubbly flow, the pressure is solved to be satisfied $\nabla^2\phi$=0. The restriction condition of the volume fraction (Eq. (18)) at the fractional step with a superscript * between N-th and (N+1)-th steps is not satisfied. Using the same method as the Projection MAC one used in the single phase flow, the pressure Poisson equation is solved to be satisfied the solenoidal condition at (N+1)-th step.

$$\frac{1}{\delta t}\frac{\partial ((f_G \bar{u}_{Gi})^{(N+1)} + (f_L \bar{u}_{Li})^*)}{\partial x_i} = \nabla^2 p \tag{20}$$

When the conservation equations of the volume fractions (Eqs. (9)(10)) are solved implicitly, gas and liquid volume fractions are expressed as

$$f_G^{(N+1)} = f_G^{(N)} - \delta t \frac{\partial (f_G \bar{u}_{Gi})^{(N+1)}}{\partial x_i} = 0, \tag{21}$$

$$f_L^* = f_L^{(N)} - \delta t \frac{\partial (f_L \bar{u}_{Li})^*}{\partial x_i} = 0. \tag{22}$$

From Eqs (20)(21)(22), the pressure Poisson equation is expressed as

$$-\frac{1}{\delta t^2}(f_G^{(N+1)} + f_L^* - 1) = \nabla^2 p. \tag{23}$$

Using the Helmholtz decomposition, the total volume flux ($f_G u_{Gi}^{(N+1)}$+$f_L\, u_L^*$) is expressed as

$$(f_G \bar{u}_{Gi})^{(N+1)} + (f_L \bar{u}_{Li})^* = \nabla \phi^* + \nabla \times \Psi^*. \tag{24}$$

The term including $\nabla \times \mathbf{\Phi}^*$ always satisfy the solenoidal condition so that only the term including ϕ is considered for the pressure Poisson equation. The pressure can be decomposed into,

$$p = p^{(A)} + p^{(B)}, \tag{25}$$

where

$$\nabla^2 p^{(A)} \neq 0, \quad \nabla^2 p^{(B)} = 0. \tag{26}$$

The pressure Poisson equation is rewritten as

$$-\frac{1}{\delta t^2}(f_G^{(N+1)} + f_L^* - 1) = \nabla^2 p^{(A)} = \frac{1}{\delta t}\nabla^2 \phi^* \tag{27}$$

From Eqs. (25)(26), the non-harmonic pressure $p^{(A)}$ is the particular solution to be satisfied $\nabla^2 p=0$. The harmonic pressure $p^{(B)}$, which is not explicitly written in Eq. (26), is the general solution and is determined by the pressure distribution on the bubble surface. In the conventional two-fluid simulation, the boundary condition of the simulation domain Γ has been considered, while the bubble interface Γ_{Bl} has been treated as the uniform and the boundary condition on Γ_{Bl} has been neglected. In order to obtain the pressure distribution near the bubbles, we must consider the harmonic pressure $p^{(B)}$ due to the pressure on the Γ_{Bl}.

If the pressure on the each bubble surface ($r=a$) is known, we can obtain the harmonic pressure $p^{(B)}$ distribution analytically and it is expressed as

$$(p^{(B)}(\mathbf{r}) - p(r)|_{r\to\infty}) = \sum_{n=0}^{\infty}\left(\frac{a}{r}\right)^{n+1}\left(p_n Y_n(\theta) + \sum_{m=1}^{n}\left(p_{nm}^{(c)} Y_{nm}^{(c)}(\theta,\phi) + p_{nm}^{(s)} Y_{nm}^{(s)}(\theta,\phi)\right)\right) \tag{28}$$

where Y_{nm}^* is the spherical harmonics and p^*_{nm} is the expansion coefficient. Therefore, the database of the pressure distribution on the bubble surface expanded by the spherical harmonics is useful for the closure problem on $p^{(B)}$, which is neglected in the conventional two-fluid model.

5.2 Problem on vorticity

From the momentum equation (Eq. (12)), the vorticity transport equation is expressed as

$$f_L \frac{D\boldsymbol{\omega}_L}{Dt} = f_L(\boldsymbol{\omega}_L \cdot \nabla)\mathbf{u}_L + (\nabla f_L) \times \left(\mathbf{g} - \frac{D\mathbf{u}_L}{Dt}\right) + \nu \nabla^2 \boldsymbol{\omega}_L, \tag{29}$$

where $\boldsymbol{\omega}_L$ is the vorticity vector. The first term of the RHS in Eq. (29) is the source term of the vorticity, which is related to the contraction and the expansion of the vortex. The second term is characteristic one of the bubbly flow and is related to the vorticity generation due to the buoyancy and the void fraction gradient. The last term is expressed the diffusion in the bulk region, while this term is related the vorticity generation in the vicinity of the bubble. In the conventional two-fluid model, the two-fluid is treated as uniform so that the boundary condition of the vorticity on the bubble interface Γ_B is neglected and it is also required to be modeled.

In the low void fraction, the vorticity is derived by the rotation of Eq. (19). The 1st term of Eq. (19) is the rotation free so that the boundary condition effect of the vorticity is related to the 2nd term $\nabla \times \mathbf{\Phi}$. As mentioned above, the harmonic pressure $p^{(B)}$ is not related to the 2nd term $\nabla \times \mathbf{\Phi}$. Therefore, the boundary conditions of the harmonic pressure and the vorticity are independent.

6. Two-Fluid Simulation (Effect of Boundary Condition)

6.1 Simulation method

6.1.1 Modeling of harmonic pressure

The simulation procedure is based on the Projection MAC method. The procedures to solve the pressure field are divided into two stages. At the first stage, the harmonic pressure is obtained by using the database of the pressure on the bubble interface. At the second stage, the pressure field is solved to satisfy the solenoidal condition of the volume flux. The second stage procedure is the same manner as the conventional two-fluid simulation thus we do not mention it here. At the first stage, the effects of the pressure drag $p^{(PD)}$ and the pressure due to the added inertia $p^{(AI)}$ are considered. To avoid the double count of the bulk pressure $p^{(BK)}$ under the treatment of the uniform flow field, its effect is subtracted at the every step.

$p^{(PD)}$ at the bubble interface is expressed as

$$p^{(PD)}(r,\theta)\Big|_{r=a} = \left|u_G - u_L^{(\infty)}\right|^2 \sum_{n=0}^{N} p_n Y_n(\theta) \tag{30}$$

where only the axisymmetric component is considered. Using the relation of $p|_{r\to\infty}\to 0$, $p^{(PD)}(r,\theta,Re)$ is expressed as

$$p^{(PD)}(r,\theta) = \left|u_G - u_L^{(\infty)}\right|^2 \sum_{n=0}^{N} \left(\frac{a}{r}\right)^{n+1} p_n Y_n(\theta) \tag{31}$$

We construct database of p_n as the function of the Reynolds number before we carry out the two-fluid simulation. $p^{(AI)}$ is expressed as

$$p^{(AI)}(\mathbf{r}) = \frac{a^3}{2}\frac{x_i}{r^3}\left(\frac{du_{Gi}}{dt} - \frac{Du_{Li}}{Dt}\right). \tag{32}$$

$p^{(BK)}$ is expressed as

$$p^{(BK)}(\mathbf{r}) = -\frac{a^3 x_j}{r^3}\left(\partial_j p^{(N)}(\mathbf{r})\Big|_{r=0}\right), \tag{33}$$

where $p^{(N)}$ is the pressure at the N-th simulation step.

6.1.2 Modeling of vorticity generation at bubble surface

The vorticity generation on the bubble surface is modeled in connection with the viscous stress generation. The pressure can be mathematically decomposed the non-harmonic part related to the solenoidal condition and the harmonic one related to the boundary condition effect because the pressure equation is linear. On the contrary, the vorticity is not able to be decomposed because the vorticity transport equation of non-linear. In the present study, the effective viscous stress of the bubbly flow is modeled using the weight function w as the function of the length from the bubble surface and is expressed as

$$\sigma_{ij}^{(E)} = (1-w)\sigma_{ij}^{(\infty)} + w\sigma_{ij}^{(PI)}, \tag{34}$$

$$w(\xi) = 1 - \frac{\xi}{\Delta x} \quad (0 \le \xi \le \Delta x), \tag{35}$$

$$w(\xi) = 0 \quad (\Delta x \le \xi), \tag{36}$$

where ξ is the length from the bubble surface and Δ_x is the grid size. $\sigma_{ij}^{(\infty)}$ and $\sigma_{ij}^{(PI)}$ are expressed as

$$\sigma_{ij}^{(\infty)} = \mu\left(\partial_i u_{Lj} + \partial_j u_{Li} - \frac{2}{3}(\partial_k u_{Lk})\delta_{ij}\right), \tag{37}$$

$$\sigma_{ij}^{(PI)} = \mu\left(\partial_i u_j^{(PI)} + \partial_j u_i^{(PI)} - \frac{2}{3}(\partial_k u_k^{(PI)})\delta_{ij}\right), \tag{38}$$

where $u^{(PI)}$ is given by the database of the velocity field around the bubble (Eq. (7)).

6.2 Simulation results

Figure 5 shows the one-dimensional vertical energy spectrum at the void fraction of 0.833%. Solid and dotted lines correspond to the DNS data without and with the grid filter operation, respectively. The '△' symbols correspond to the results obtained by the conventional two-fluid model. The '○' symbols correspond to the results obtained by the present model, where the SGS stress (the Reynolds stress) and the effects of the boundary condition are considered. It is seen from Fig. 5 The turbulent energy spectrum obtained by the conventional two-fluid model show the considerable difference with the DNS results, while the present model reproduces the DNS one well. Therefore, it is important to consider not only the SGS stress (the Reynolds stress) but also the effects of the boundary condition in the multiscale modeling of the bubbly flow.

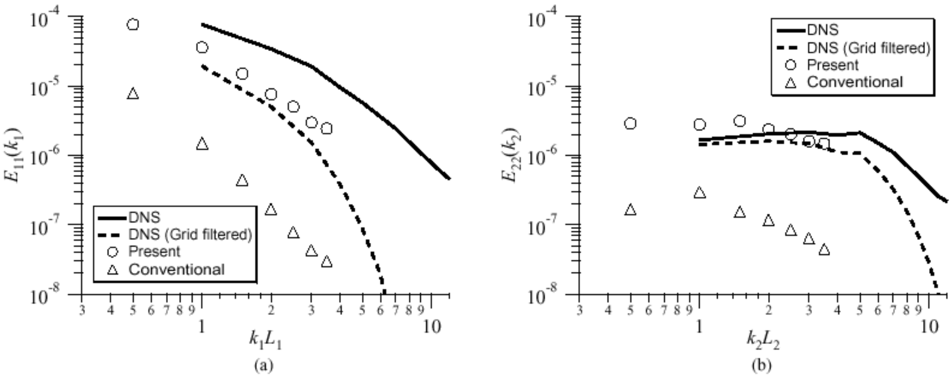

Fig. 5 One-dimensional vertical energy spectrum versus wave number at the void fraction of 0.833%.

((a) Vertical component, (b) Horizontal component)

7. Conclusions

The DNS and the two-fluid simulation are carried out in order to conduct the multiscale modeling of the bubbly flow.

The energy spectrum distribution, which is related to the turbulent structure due to the motion of the rising packed bubbles, is obtained by the DNS of the multi-bubble system.

The new multiscale modeling of the bubbly flow for the two-fluid model is conducted. The constitutive equations, where the SGS stresses and the boundary conditions of the pressure and the vorticity on the interface are taken into account, are derived. The turbulent energy spectrum obtained by the present two-fluid model reproduces the DNS result well, while the result by the conventional two-fluid model, where the SGS stress and the boundary conditions on the interface are neglected, show considerable difference with the DNS one.

References

(1) Bardina, J., Feriger, J.H. and Reynolds, W.C., 1983, Report No. TF-19, Stanford Univ.

(2) Batchelor, G.K., 1967, *'An Introduction to Fluid Dynamics,'* (Cambridge University Press).

(3) Chandrasekhar, S., 1961, *'Hydrodynamic and hydromagnetic stability,'* (Oxford Univ. Press).

(4) Drew, D.A., 1983, *Annu. Rev. Fluid Mech.*, **15**, 261.

(5) Ishii, M, 1975, *'Thermo-fluid Dynamics Theory of Two-phase Flow,'* (Eyrolles, Paris).

(6) Liu, S., Meneveau, C. and Katz, J., 1994, *J. Fluid Mech.*, **275**, 83.

(7) Matsumoto, Y., Nishikawa, H. and Ohashi, H., 1988, *JSME Int. J, Ser. II*, **31**, 652.

(8) Murai, Y. and Matsumoto, Y., 1996, *Proc. of ASME FED*, **236-1**, 67.

(9) Schiller, L. and Naumann, A.Z., 1933, *Z. Ver. Dtsch. Ing*, **77**, 318.

(10) Smagorinsky, J., 1963, *Mon. Weath. Rev.*, **91**, 99.

(11) Sugiyama, K., Takagi, S. and Matsumoto, Y., 2000, *Proc. of ASME FEDSM'00*, FEDSM00-11141 (CDROM).